International Journal of Solids and Structures 45 (2008) 6114–6132

Contents lists available at ScienceDirect

International Journal of Solids and Structures

journal homepage: www.elsevier.com/locate/ijsolstr

In-plane free vibration of a single-crystal silicon ring

Chia-Ou Chang [a,*], Guo-En Chang [a], Chan-Shin Chou [a], Wen-Tien Chang Chien [b], Po-Chih Chen [a]

[a] Institute of Applied Mechanics, National Taiwan University, No.1, Sec. 4, Roosevelt Road, Taipei, 106, Taiwan, ROC
[b] Department of Information Management, Fooyin University, Ta-Liao, Kaohsiung, Taiwan, ROC

ARTICLE INFO

Article history:
Received 29 January 2008
Received in revised form 11 July 2008
Available online 19 August 2008

Keywords:
Single-crystal silicon
Natural frequencies
Anisotropic effect
Frequency splitting

ABSTRACT

In this paper the natural frequencies and the associated mode shapes of in-plane free vibration of a single-crystal silicon ring are analyzed. It is found that the Si(111) ring is two-dimensionally isotropic in the (111) plane for elastic constants but three-dimensionally anisotropic, while the Si(100) ring is fully anisotropic. Hamilton's principle is used to derive the equations of vibration, which is a set of partial differential equations with coefficients being periodic in polar variable. Expressing the radial and tangential displacements in sinusoidal form with non-predetermined amplitudes, and through the integration with respect to the circumferential variable, the original governing equations in partial differential form can be converted into the amplitude equations in ordinary differential form. The exact expressions for frequencies and mode shapes are obtained. It is found that for Si(100) rings the frequencies of a pair of modes, which are equal for an isotropic ring, split due to the anisotropic effect only for the second in-plane vibration mode. The phenomena of frequency splitting and degenerate modes can be proved either based on the conservation of averaged mechanical energy or by the concept of crystallographic symmetry groups. When the single-crystal silicon is replaced by the polycrystalline silicon, which is isotropic in elastic constants, the derived equations for frequencies correctly predict the vanishing of the phenomenon of frequency splitting.

1. Introduction

The rapid development of micro-engineering techniques makes the miniaturization of actuators and sensors more and more feasible. Gyroscopes are used to measure the rotation rate or the angles of turn. Micro-gyroscopes are needed, for the purposes of cost and space reduction in many applications, for instance, inertial mousses in computers, man–machine interaction in the field of virtual reality, and other applications where the orientations need to be measured, such as unmanned vehicle or robots. There are several different kinds of micro-gyroscopes reported in the literatures. The ring-like components (Hopkins, 1997; Putty and Najafi, 1994) is of great interest, because its center of mass remains unchanged during operation so that the rigid-body effect is removed.

Although polycrystalline silicon is isotropic in mechanical property, but due to its inherent nature of having higher internal damping than single-crystal silicon, most ring gyroscopes are made of the latter. He and Najafi (2002) reported that rings made of single-crystal silicon wafer have higher quality factor (Q) than those made of poly-crystalline silicon wafer (Putty and Najafi, 1994; Ayazi and Najafi, 2001). The above-mentioned references focused on the system design and performance testing of the ring gyroscope, rather than the frequency analysis of vibrating rings. Perfect circular rings made from isotropic material, such as metals or Si(111) (single-crystal silicon wafer cut in the (111) plane), have degenerated pairs of vibration modes. This means that the two modes for any pair have equal natural frequencies. If one of the two degenerate modes is used as the driving mode and the other as the sensing mode, the sensitivity of measurement is greatly increased, because the vibration amplitudes of these two modes are almost of the same order.

* Corresponding author. Tel.: +886 2 33665626; fax: +886 2 23639290.
E-mail address: changco@spring.iam.ntu.edu.tw (C.-O. Chang).

0020-7683/$ - see front matter © 2008 Elsevier Ltd. All rights reserved.
doi:10.1016/j.ijsolstr.2008.07.033

In order to avoid the loss of signal from the mechanical element (that is, the vibrating ring) to the pick-off electric-circuit element due to the distance transmission, it is a trade off to combine the ring and the electric-circuit in a single silicon chip. Moreover, single-crystal silicon wafers are usually chosen to be of the (100) orientation rather the (111) one, because Si(100) has much faster etching rate than Si(111) and is commonly used in the semiconductor industry. However, rings made from silicon in the (100) plane are anisotropic in elastic moduli; this anisotropy causes the two frequencies of a pair of similar modes, which are equal for isotropic rings (Love, 1944), to split.

Although the free vibration of a circular ring had been widely studied, most of them focused on isotropic rings rather than anisotropic ones. For example, Kirkhope (1976) studied the vibration of non-rotating circular ring including the effects of shear deformation and rotatory inertia; Carrier (1945) derived the governing equations of free vibration for rotating rings; Bickford and Reddy (1985) numerically analyzed the similar problem including the effects of inextensional, shear deformation, and rotatory inertia; Tang and Bert (1987) studied the out-of-plane vibration of thick isotropic rings; Hwang et al. (1999) investigated the effect of the variation of in-plane geometric profile of an isotropic ring on the frequency splitting. Some researchers investigated anisotropic rings. For example, Eley et al. (1999) studied the directional variations of elastic moduli for single-crystal silicon in the (100) plane, and the additional variations in the elastic moduli for the planes misaligned from the (111) and (100) planes.

The aim of this paper is to analyze the effect of anisotropic elastic constants on the natural frequencies of a ring made from a single-crystal silicon wafer. The effect of anisotropy can be accounted for in the expression of strain energy; therefore, the accuracy of the solution of the frequencies depends on the amount of deviation of the approximate formulation of strain energy to the exact one. Eley et al. (1999) borrowed the strain energy expression of anisotropic materials from isotropic ones as used by Kirkhope (1976, 1977) and replaced the constant Young's modulus by the one which is function of the circumferential variable of the ring. In so doing, they considered each differential volume of the ring in cylindrical coordinates as an isotropic body; therefore, his expression for strain energy is just an approximate one. In addition, they assumed that the mode shapes of pairs of similar modes of an anisotropic ring are the same as those of an isotropic ring to facilitate the calculation of the natural frequencies. In fact, it is still unknown whether the amplitude ratio of radial to tangential displacements of anisotropic rings remains the same as that of isotropic rings. To account for the anisotropic effect, we determine the strain energy of anisotropic rings in a theoretically correct form, in which each differential volume of the ring is actually considered as anisotropic elastic body. We use Hamilton's principle to derive the equations of motion of the ring, which is a set of partial differential equations with coefficients varying in polar variable. These equations are then converted to a set of ordinary differential equations in terms of modal amplitudes by the assumed-mode method. By solving the amplitude equations, the explicit forms of natural frequencies and the amplitude ratio of radial to tangential displacements are found. The result indicates that the natural frequencies of pairs of similar modes of the anisotropic Si(100) ring split only for the second in-plane vibration mode. The theoretically-rigorous explanations of the phenomena of frequency splitting and degenerated modes are given based on the conservation of averaged mechanical energy. In some cases, the degenerated modes can also be easily interpreted from the crystallographic symmetry elements. In addition, we find that the mode shapes of vibration are dependent on the geometrical size of the ring regardless of the material properties of the ring.

2. Anisotropic property of single-crystal silicon

Single-crystal silicon belongs to the face-centered cubic diamond structure and its point symmetry group is of m3m class (Ashcroft and Mermin, 1975; Shuvalov, 1981). The silicon wafers nominally cut parallel to the (111) and (100) orientations are usually manufactured as the substrates or the main bodies of the micro-devices. Single-crystal silicon of (111) orientation has isotropic mechanical properties. On the other hand, silicon of (100) orientation has anisotropic mechanical properties but it has chemical etching rates about four hundred times faster than Si(111) (Elwenspoek and Jansen, 1998). This is the main reason that Si(100) wafers are commonly used in the CMOS industries rather than Si(111) ones because of the advantage of easy-manufacture.

The anisotropic effect is embodied in the strain energy of the elastic ring. In order to obtain the exact expression for strain energy of each differential volume of the ring in cylindrical coordinates, we first have to find the proper stiffness matrices that relate stress to strain through the linear constitutive equation, for Si(100) and Si(111).

2.1. The stiffness matrix of Si(100)

Consider a ring, as shown in Fig. 1, of diameter a, width h, and thickness b respectively. Let Z axis be the direction perpendicular to the ring surface and θ the angle measured form the X axis. The stress tensor σ_{ij}, strain tensor ε_{kl}, and the constitutive equation $\sigma_{ij} = C_{ijkl}\varepsilon_{kl}$ can be expressed in the matrix-vector form as $\boldsymbol{\sigma}_{6\times1} = \mathbf{C}_{6\times6}\,\boldsymbol{\varepsilon}_{6\times1}$, if we rewrite the matrix and vector subscripts in terms of the tensor subscripts as

$$1 \to 11, \quad 2 \to 22, \quad 3 \to 33, \quad 4 \to 23, \quad 5 \to 31, \quad \text{and} \quad 6 \to 12 \tag{1}$$

such that $\sigma_{12} \to \sigma_6$, $\varepsilon_5 \to \varepsilon_{31}$, and $C_{14} \to C_{1123}$. Because the unit cell of a single-crystal silicon is a face-centered cubic lattice, it is well known that the stiffness matrix $\mathbf{C}_{(100)}$ of Si(100) with respect to a fixed Cartesian coordinate system is (Nye, 1957; Royer and Dieulesaint, 2000)

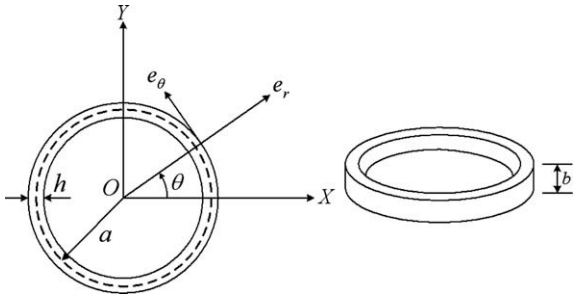

Fig. 1. The dimensions of the ring.

$$\mathbf{C}_{(100)} = \begin{bmatrix} C_{11} & C_{12} & C_{12} & 0 & 0 & 0 \\ C_{12} & C_{11} & C_{12} & 0 & 0 & 0 \\ C_{12} & C_{12} & C_{11} & 0 & 0 & 0 \\ 0 & 0 & 0 & C_{44} & 0 & 0 \\ 0 & 0 & 0 & 0 & C_{44} & 0 \\ 0 & 0 & 0 & 0 & 0 & C_{44} \end{bmatrix} \tag{2a}$$

where the values of elastic constants are given as follows (Shuvalov, 1981; Wortman and Evans, 1965; Brantley, 1973):

$$C_{11} = 165.7 \text{ GPa}, \quad C_{12} = 63.9 \text{ GPa}, \quad C_{44} = 79.6 \text{ GPa}. \tag{2b}$$

In order to express strain energy of differential volumes in cylindrical coordinates, the stiffness matrix referred to a Cartesian coordinate system should be transformed by using the tensor transformation equation:

$$C'_{ijkl} = a_{im}a_{jn}a_{ko}a_{lp}C_{mnop} \tag{3}$$

into one referred to the cylindrical coordinate system as

$$\mathbf{C}'_{(100,\theta)} = \begin{bmatrix} C'_{11} & C'_{12} & C'_{13} & 0 & 0 & C'_{16} \\ C'_{12} & C'_{11} & C'_{13} & 0 & 0 & C'_{26} \\ C'_{13} & C'_{13} & C'_{33} & 0 & 0 & 0 \\ 0 & 0 & 0 & C'_{44} & 0 & 0 \\ 0 & 0 & 0 & 0 & C'_{44} & 0 \\ C'_{16} & C'_{26} & 0 & 0 & 0 & C'_{66} \end{bmatrix} \tag{4a}$$

where the non-zero elements of matrix $\mathbf{C}'_{(100,\theta)}$ are given in Appendix A. The compliance matrix $\mathbf{S}$ relates the strain vector $\boldsymbol{\varepsilon}$ to the stress vector $\boldsymbol{\sigma}$ as $\boldsymbol{\varepsilon} = \mathbf{S}\boldsymbol{\sigma}$. It is obvious that $\mathbf{S} = \mathbf{C}^{-1}$. The compliance matrix of Si(100) referred to the cylindrical coordinate system r,θ,z (with the unit radial vector $\mathbf{e}_r$ being an angle θ from the positive X axis in the counterclockwise sense, as shown in Fig. 1) appears in constitutive equation as

$$\begin{Bmatrix} \varepsilon_1 \\ \varepsilon_2 \\ \varepsilon_3 \\ \varepsilon_4 \\ \varepsilon_5 \\ \varepsilon_6 \end{Bmatrix} = \begin{bmatrix} S'_{11} & S'_{12} & S'_{13} & 0 & 0 & S'_{16} \\ S'_{12} & S'_{11} & S'_{13} & 0 & 0 & S'_{26} \\ S'_{13} & S'_{13} & S'_{33} & 0 & 0 & 0 \\ 0 & 0 & 0 & S'_{44} & 0 & 0 \\ 0 & 0 & 0 & 0 & S'_{44} & 0 \\ S'_{16} & S'_{26} & 0 & 0 & 0 & S'_{66} \end{bmatrix} \begin{Bmatrix} \sigma_1 \\ \sigma_2 \\ \sigma_3 \\ \sigma_4 \\ \sigma_5 \\ \sigma_6 \end{Bmatrix} \text{ or } \boldsymbol{\varepsilon} = \mathbf{S}'_{(100,\theta)}\boldsymbol{\sigma} \tag{4b}$$

where the non-zero entries elements are also given in Appendix A. Consider a strip of rectangular cross-section with its longitudinal axis parallel to the r axis and the other two transverse axes parallel to the θ and z axes. The two in-plane elastic moduli can be obtained from the tensile deformed state: one is subjected to the axial load $\boldsymbol{\sigma} = (\sigma_1,0,0,0,0,0)^{\mathbf{T}}$, and the other is subjected to the load $\boldsymbol{\sigma} = (0,\sigma_2,0,0,0,0)^{\mathbf{T}}$. From Eq. (4b), the two in-plane Young's moduli are found to be equal and are denoted by $E_{\text{in}}(\theta)$, which depends on the θ variable, as

$$\frac{1}{E_{\text{in}}(\theta)} = S'_{11} = S_{11} - \frac{1}{4}(1-\cos 4\theta)\left(S_{11} - S_{12} - \frac{S_{44}}{2}\right) = S_{11} - 2\left(S_{11} - S_{12} - \frac{1}{2}S_{44}\right)F(\theta) \tag{5a}$$

where $F(\theta) = \frac{1}{8}(1-\cos 4\theta)$. The out-of-plane Young's modulus is obtained by letting the strip that is subjected to the load $\boldsymbol{\sigma} = (0,0,\sigma_3,0,0,0)^{\mathbf{T}}$ equal to

$$\frac{1}{E_{\text{out}}} = S'_{33} = S_{11} \tag{5b}$$

which is independent of the θ variable. Applying an in-plane shear loading $\boldsymbol{\sigma} = (0,0,0,0,0,\sigma_6)^{\mathbf{T}}$ to the strip, we get from Eq. (4b) that $\varepsilon_6 = S'_{66}\sigma_6$, then the in-plane shear modulus is

$$\frac{1}{G_{\text{in}}(\theta)} = S'_{66} = S_{44} + (1-\cos 4\theta)\left(S_{11} - S_{12} - \frac{S_{44}}{2}\right) = S_{44} + 8\left(S_{11} - S_{12} - \frac{1}{2}S_{44}\right)F(\theta). \tag{5c}$$

If we apply the out-of-plane shear forces $\boldsymbol{\sigma} = (0,0,0,\sigma_4,0,0)^{\mathbf{T}}$ and $\boldsymbol{\sigma} = (0,0,0,0,\sigma_5,0)^{\mathbf{T}}$ to the strip, the out-of-plane shear moduli for these two loading states obtained from Eq. (4b) are the same as

$$\frac{1}{G_{\text{out}}} = S'_{44} = S_{44} \tag{5d}$$

Eley et al. (1999) got the in-plane shear modulus for Si(100) in the form

$$\frac{1}{G_{\text{in}}(\theta)} = S_{44} + 4\left(S_{11} - S_{12} - \frac{S_{44}}{2}\right)F(\theta). \tag{5e}$$

The slight difference between Eqs. (5c) and (5e) is that there is a factor of eight in the second term of the rightmost side of our Eq. (5c) and this factor is changed to four in Eq. (5e). This difference is visualized by graphs plotted in Fig. 2.

However, Eq. (5c) agrees with Wortman and Evans' results (1965) which are expressed as a function of directional cosines, as shown in Appendix B. The graphic representation of elastic and shear moduli of Si(100) as a function of polar coordinate θ, as shown in Fig. 3 (Each dashed circle in Fig. 3 represents a contour line and all the points on this line have the same value of shear or Young's modulus) indicates that both elastic and shear moduli are direction-dependent in the (100) plane, but are constant in the direction normal to the (100) plane. Namely, Si(100) is fully anisotropic. In addition, if the circular ring is made from polycrystalline silicon (i.e. fully isotropic material), it must satisfy the condition $C_{44} = (C_{11} - C_{12})/2$, and the factor $(S_{11} - S_{12} - S_{44}/2)$ in Eqs. (5a) and (5c) becomes zero according to Eq. (A3). Then the in-plane and out-of-pane elastic and shear moduli of Si(100) will reduce to

$$\begin{cases} E_{\text{in}} = E_{\text{out}} = \frac{(C_{11}-C_{12})(C_{11}+2C_{12})}{C_{11}+C_{12}} \\ G_{\text{in}} = G_{\text{out}} = \frac{(C_{11}-C_{12})}{2} \end{cases} \tag{6}$$

which shows that the polycrystalline silicon is fully isotropic as expected.

2.2. The stiffness matrix of Si(111)

The stiffness matrix of Si(111) can be obtained by performing tensor transformation on the Si(100) stiffness matrix. Let $\bar{X}\bar{Y}\bar{Z}$ be the rectangular coordinate system with $\bar{Z}$ axis being perpendicular to the (111) plane, $\bar{X}$ axis in the $[\bar{1}\,\bar{1}\,2]$ direction, $\bar{Y}$ axis in the $[1\,\bar{1}\,0]$ direction, and both $\bar{X}$ and $\bar{Y}$ axes are lying on the (111) plane as shown in Fig. 4. The components of any vector expressed in the $\bar{X}\bar{Y}\bar{Z}$ coordinate system are related to those expressed in the XYZ coordinate system by

$$\begin{Bmatrix} \bar{X} \\ \bar{Y} \\ \bar{Z} \end{Bmatrix} = \mathbf{A}\begin{Bmatrix} X \\ Y \\ Z \end{Bmatrix}, \quad \text{where} \quad \mathbf{A} = \begin{bmatrix} -\frac{1}{\sqrt{6}} & -\frac{1}{\sqrt{6}} & \frac{2}{\sqrt{6}} \\ \frac{1}{\sqrt{2}} & \frac{1}{\sqrt{2}} & 0 \\ \frac{1}{\sqrt{3}} & \frac{1}{\sqrt{3}} & \frac{1}{\sqrt{3}} \end{bmatrix} \tag{7}$$

Performing tensor transformation according to Eq. (3) and using Eqs. (2) and (7), the stiffness matrix of Si(111) can be obtained as

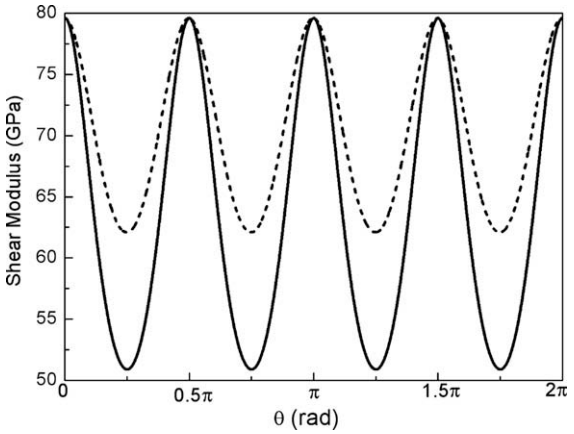

Fig. 2. The shear modulus of Eq. (5c) (the solid line) and Eq. (5e) (the dashed line).

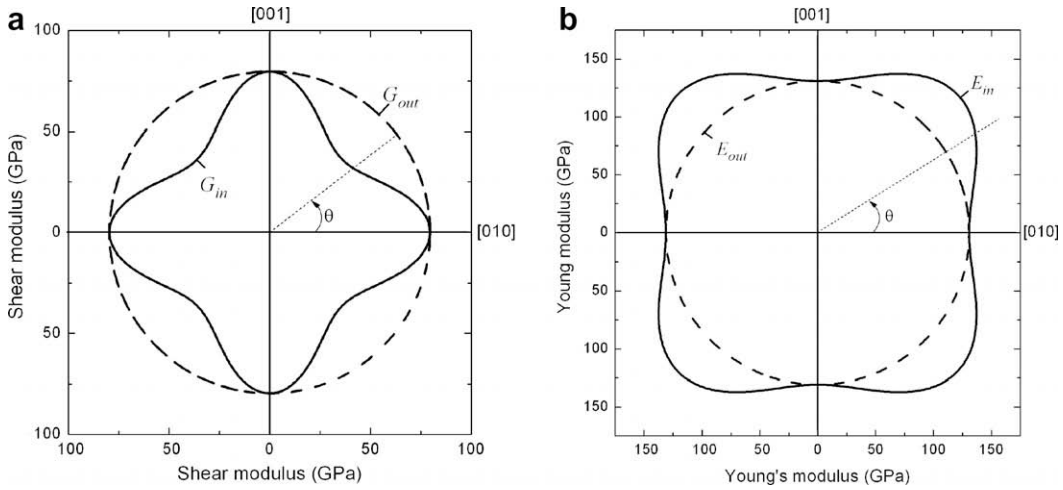

Fig. 3. (a) In-plane and out-of-plane shear moduli, G_{in} and G_{out}, of Si(1 0 0) as function of polar coordinate θ. (b) In-plane and out-of-plane elastic moduli, E_{in} and E_{out}, of Si(1 0 0) as function of θ. (Each dashed circle represents a contour line).

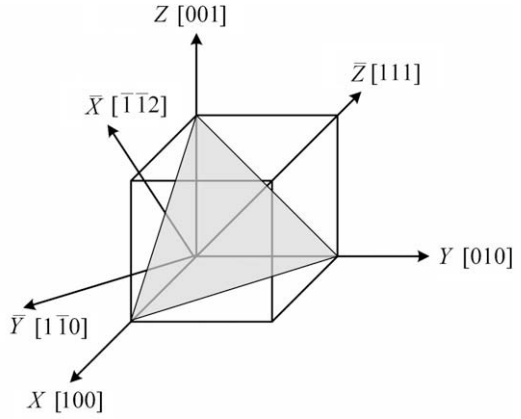

Fig. 4. Configurations of coordinate systems for Si(1 1 1).

$$\mathbf{C}_{(1\,1\,1)} = \begin{bmatrix} \overline{C}_{11} & \overline{C}_{12} & \overline{C}_{13} & 0 & \overline{C}_{15} & 0 \\ \overline{C}_{12} & \overline{C}_{11} & \overline{C}_{13} & 0 & -\overline{C}_{15} & 0 \\ \overline{C}_{13} & \overline{C}_{13} & \overline{C}_{33} & 0 & 0 & 0 \\ 0 & 0 & 0 & \overline{C}_{44} & 0 & -\overline{C}_{15} \\ \overline{C}_{15} & -\overline{C}_{15} & 0 & 0 & \overline{C}_{44} & 0 \\ 0 & 0 & 0 & -\overline{C}_{15} & 0 & \overline{C}_{66} \end{bmatrix} \tag{8}$$

where the non-zero entries of $\mathbf{C}_{(1\,1\,1)}$ are given in Appendix C. Let $r\theta Z'$ be the cylindrical coordinates obtained by rotating the rectangular coordinate system $\bar{X}\bar{Y}\bar{Z}$ about the $\bar{Z}$ axis by an angle θ. Then the stiffness matrix referring to this cylindrical coordinates is

$$\mathbf{C}_{(1\,1\,1,\theta)} = \begin{bmatrix} \overline{C}'_{11} & \overline{C}'_{12} & \overline{C}'_{13} & -\overline{C}'_{24} & \overline{C}'_{15} & 0 \\ \overline{C}'_{12} & \overline{C}'_{11} & \overline{C}'_{13} & \overline{C}'_{24} & -\overline{C}'_{15} & 0 \\ \overline{C}'_{13} & \overline{C}'_{13} & \overline{C}'_{33} & 0 & 0 & 0 \\ -\overline{C}'_{24} & \overline{C}'_{24} & 0 & \overline{C}'_{44} & 0 & -\overline{C}'_{15} \\ \overline{C}'_{15} & -\overline{C}'_{15} & 0 & 0 & \overline{C}'_{44} & -\overline{C}'_{24} \\ 0 & 0 & 0 & -\overline{C}'_{15} & -\overline{C}'_{24} & \overline{C}'_{66} \end{bmatrix} \tag{9a}$$

Inversing this stiffness matrix gives the compliance matrix as

$$\mathbf{S}_{(1\,1\,1,\theta)} = \begin{bmatrix} \bar{S}'_{11} & \bar{S}'_{12} & \bar{S}'_{13} & -\bar{S}'_{24} & \bar{S}'_{15} & 0 \\ \bar{S}'_{12} & \bar{S}'_{11} & \bar{S}'_{13} & \bar{S}'_{24} & -\bar{S}'_{15} & 0 \\ \bar{S}'_{13} & \bar{S}'_{13} & \bar{S}'_{33} & 0 & 0 & 0 \\ -\bar{S}'_{24} & \bar{S}'_{24} & 0 & \bar{S}'_{44} & 0 & -\bar{S}'_{15} \\ \bar{S}'_{15} & -\bar{S}'_{15} & 0 & 0 & \bar{S}'_{44} & -\bar{S}'_{24} \\ 0 & 0 & 0 & -\bar{S}'_{15} & -\bar{S}'_{24} & \bar{S}'_{66} \end{bmatrix} \tag{9b}$$

where the non-zero entries of matrices $\mathbf{C}_{(1\,1\,1,\theta)}$ and $\mathbf{S}_{(1\,1\,1,\theta)}$ are given in Appendix C. From Eq. (9b) the in-plane and out-of-plane elastic and shear moduli of Si(1 1 1) are found to be

$$E_{\text{in}} = \frac{1}{\bar{S}'_{11}} = \frac{[2\bar{C}_{13}^2 - \bar{C}_{33}(\bar{C}_{11}+\bar{C}_{12})][\bar{C}_{44}(\bar{C}_{11}-\bar{C}_{12}) - 2\bar{C}_{15}^2]}{\bar{C}_{15}^2\bar{C}_{33} + \bar{C}_{44}(\bar{C}_{13}^2 - \bar{C}_{11}\bar{C}_{33})} \tag{10a}$$

$$E_{\text{out}} = \frac{1}{\bar{S}'_{33}} = \frac{\bar{C}_{33}(\bar{C}_{11}+\bar{C}_{12}) - 2\bar{C}_{13}^2}{\bar{C}_{11}+\bar{C}_{12}} \tag{10b}$$

$$G_{\text{in}} = \frac{1}{\bar{S}'_{66}} = \frac{\bar{C}_{44}\bar{C}_{66} - \bar{C}_{15}^2}{\bar{C}_{44}} \tag{10c}$$

$$G_{\text{out}} = \frac{1}{\bar{S}'_{44}} = \frac{\bar{C}_{44}(\bar{C}_{11}-\bar{C}_{12}) - 2\bar{C}_{15}^2}{\bar{C}_{11}-\bar{C}_{12}} \tag{10d}$$

These moduli can be calculated from the known values of C_{11},C_{12}, andC_{44} given in Eq. (2b). They are E_{in} = 169.10 GPa, E_{out} = 187.85 GPa, G_{in} = 67.00 GPa, and G_{out} = 57.85 GPa. The results from Eq. (10) indicate that $E_{\text{in}} \neq E_{\text{out}}$ and $G_{\text{in}} \neq G_{\text{out}}$, they also show that both the elastic and shear moduli of Si(1 1 1) are not functions of θ, which means that Si(1 1 1) is mechanically isotropic in-plane, but anisotropic out-of-plane.

3. Equations of vibration

We adopt the hypothesis (that is, the plane of the cross-section remains plane which is perpendicular to the longitudinal axis during deformation, and there is no Poisson's effect) made in the theory of the Euler beam to analyze the silicon ring as shown in Fig. 1. The cross section of the ring is shown in Fig. 5, where u, v, and w are the radial, tangential, and out-of-plane displacements of the central line of the ring, respectively; a is the radius of the central line; ϕ_i is the rotation angle about the z-axis due to in-plane bending; $\bar{r}$ is the radial distance of any point P in the ring to the rectangular coordinate system x, y, z with the origin located at the central line; and x is the axis parallel to the unit vector $\mathbf{e}_r$ as shown in Fig. 1 so we have $r = a + \bar{r}$. If only the in-plane flexural vibration is considered, then the displacement field of the ring can be written as (Kim and Chung, 2002)

$$\begin{aligned} &U_r(\theta,t) = u(\theta,t), \quad U_\theta(\theta,t) = v(\theta,t) + \bar{r}\phi_i(\theta,t), \\ &U_z = 0, \quad \phi_i = \frac{1}{a}(v - \partial u/\partial\theta) \end{aligned} \tag{11}$$

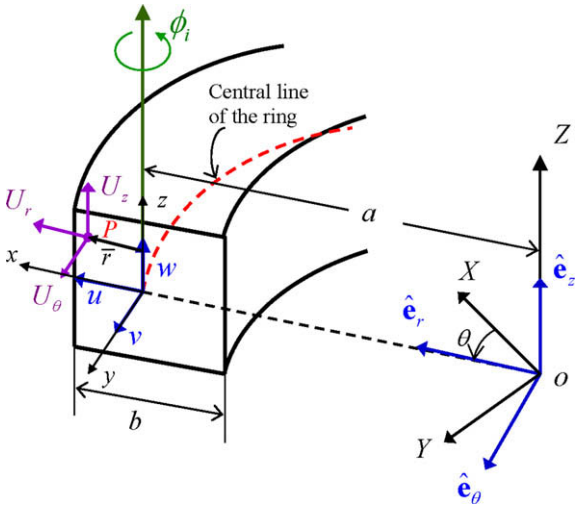

Fig. 5. Coordinate systems and displacements of the ring.

If the amplitude of vibration is considered to be small, we need only the linear strain fields (Lee and Chao, 2000) which can be obtained, by using the displacement fields given in Eq. (11), as

$$\begin{aligned}
\varepsilon_{rr} &= \frac{\partial U_r}{\partial r} = 0 \\
\varepsilon_{\theta\theta} &= \frac{U_r}{r} + \frac{1}{r}\frac{\partial U_\theta}{\partial \theta} = \frac{u}{a} + \frac{1}{a}\left[\frac{\partial v}{\partial \theta} + \frac{\bar{r}}{a}\left(\frac{\partial v}{\partial \theta} - \frac{\partial^2 u}{\partial \theta^2}\right)\right] \\
\gamma_{r\theta} &= \frac{1}{r}\frac{\partial U_r}{\partial \theta} + \frac{\partial U_\theta}{\partial r} - \frac{U_\theta}{r} = 0 \\
\varepsilon_{zz} &= \gamma_{\theta z} = \gamma_{rz} = 0
\end{aligned} \tag{12}$$

Under the assumptions of small deformation and linear stress–strain relationship the elastic stain energy density (Mal and Singh, 1991; Reismann and Pawlik, 1980) of a Si(100) ring is

$$V_r = \frac{1}{2}\boldsymbol{\varepsilon}^{\mathrm{T}}\mathbf{C}\boldsymbol{\varepsilon} = \frac{1}{2}[0 \quad \varepsilon_{\theta\theta} \quad 0 \quad 0 \quad 0 \quad 0]\begin{bmatrix} C'_{11} & C'_{12} & C'_{13} & 0 & 0 & C'_{16} \\ C'_{12} & C'_{11} & C'_{13} & 0 & 0 & C'_{26} \\ C'_{13} & C'_{13} & C'_{33} & 0 & 0 & 0 \\ 0 & 0 & 0 & C'_{44} & 0 & 0 \\ 0 & 0 & 0 & 0 & C'_{44} & 0 \\ C'_{16} & C'_{26} & 0 & 0 & 0 & C'_{66} \end{bmatrix}\begin{bmatrix} 0 \\ \varepsilon_{\theta\theta} \\ 0 \\ 0 \\ 0 \\ 0 \end{bmatrix} = \frac{1}{2}C'_{11}\varepsilon^2_{\theta\theta} \tag{13}$$

where $C'_{11} = \frac{1}{4}[3C_{11} + C_{12} + 2C_{44} + (C_{11} - C_{12} - 2C_{44})\cos 4\theta]$.

Eq. (13) is the strain energy density for any differential volume $r\mathrm{d}r\mathrm{d}\theta\mathrm{d}z(= a\mathrm{d}\bar{r}\mathrm{d}\theta\mathrm{d}z)$ which is considered as an anisotropic body. If, for the purpose of reducing the complexity of analysis, we may adopt an approximation in which the differential volume of the ring is considered as an isotropic body and the Young's modulus E in that differential volume is constant and given by Eq. (5a); then the widely used equation expressing the strain energy density for isotropic body is (Kirkhope, 1977)

$$V_r = \frac{1}{2}E(\theta)\varepsilon^2_{\theta\theta} = \frac{1}{2}\left(\frac{1}{[S_{11} - 2(S_{11} - S_{12} - S_{44}/2)F(\theta)]}\right)\varepsilon^2_{\theta\theta} \tag{14}$$

where $F(\theta) = (1 - \cos 4\theta)/8$. Notice that although the Young's modulus is constant in each differential volume, each differential volume has its own Young's modulus, because $E(\theta)$ is function of θ, that is, it depends on the orientation of the differential volume. The graphs of these two different strain energy densities described by Eqs. (13) and (14) versus the circumferential variable θ are plotted in Fig. 6. This remarkable difference in magnitude of these two energy densities reveals that the strain energy density, Eq. (14), of an isotropic differential volume adopted by Eley et al. (1999) is not close to the exact one, Eq. (13), of an anisotropic differential volume. Furthermore, the θ dependency appearing in the denominator of Eq. (14) increases the extent of difficulty in the subsequent analysis. Therefore, Eq. (13), which correctly accounts for the anisotropic property of differential volume of the ring, is used for frequency and amplitude analysis of the silicon ring later.

The strain energy of the Si(100) ring obtained by the using Eq. (12) is

$$V_r = \int_0^{2\pi}\int_{-\frac{b}{2}}^{\frac{b}{2}}\int_{-\frac{h}{2}}^{\frac{h}{2}}\frac{a}{2}\boldsymbol{\varepsilon}^{\mathrm{T}}\mathbf{C}\boldsymbol{\varepsilon}\mathrm{d}\bar{r}\mathrm{d}z\mathrm{d}\theta = \int_0^{2\pi}\frac{bh}{96a^3}\left\{\begin{array}{l}[3C_{11} + C_{12} + 2C_{44} + (C_{11} - C_{12} - 2C_{44})\cos 4\theta] \\ \quad \times[12a^2u^2 + 24a^2uv' + (12a^2 + h^2)v'^2 - 2h^2v'u'' + h^2u''^2]\end{array}\right\}\mathrm{d}\theta \tag{15}$$

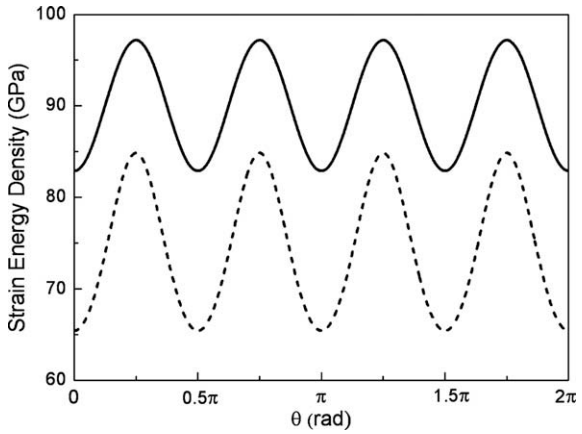

Fig. 6. The graphs of strain energy densities vs. θ. Solid line: Eq. (13). Dashed line: Eq. (14).

The position vector of any point P of the ring in the deformed state found by using Eq. (11) is

$$\vec{r}_p = (a+\bar{r}+U_r)\,\vec{e}_r + U_\theta\,\vec{e}_\theta = (a+\bar{r}+u)\,\vec{e}_r + \left[v+\frac{\bar{r}}{a}\left(v-\frac{\partial u}{\partial\theta}\right)\right]\vec{e}_\theta \tag{16}$$

Then the velocity at this point is

$$\vec{v}_p = \frac{\partial\,\vec{r}_p}{\partial t} = \dot{u}\,\vec{e}_r + \frac{(a+\bar{r})\dot{v}-\bar{r}\dot{u}'}{a}\,\vec{e}_\theta \tag{17}$$

where the dot and prime denote the derivative with respect to time and θ, respectively.

The kinetic energy of the ring with mass density ρ is

$$K_r = \int_0^{2\pi}\int_{-\frac{b}{2}}^{\frac{b}{2}}\int_{-\frac{h}{2}}^{\frac{h}{2}}\frac{\rho}{2}a(\vec{v}_p\cdot\vec{v}_p)\mathrm{d}\bar{r}\mathrm{d}z\mathrm{d}\theta = \int_0^{2\pi}\frac{bh\rho[12a^2\dot{u}^2+(12a^2+h^2)\dot{v}^2-2h^2\dot{v}\dot{u}'+h^2\dot{u}'^2]}{24a}\mathrm{d}\theta \tag{18}$$

The equations of motion are derived by using Hamilton's principle

$$\int_{t_0}^{t_1}(\delta V_r-\delta K_r)\mathrm{d}t = 0 \tag{19}$$

Substituting Eqs. (15) and (18) into Eq. (19) yields

$$\int_{t_0}^{t_1}(\delta V-\delta K)\mathrm{d}t = \int_{t_0}^{t_1}\int_0^{2\pi}(Y_1)\delta u\mathrm{d}\theta\mathrm{d}t + \int_{t_0}^{t_1}\int_0^{2\pi}(Y_2)\delta v\mathrm{d}\theta\mathrm{d}t = 0 \tag{20}$$

Since the variation of displacements, δu and δv, can be chosen arbitrarily, the existence of Eq. (20) requires the coefficients of δu and δv to be zero, that is

$$\begin{aligned} Y_1 = {} & \frac{bh}{96a^3}\{96a^4\rho\ddot{u}+24a^2[3C_{11}+C_{12}+2C_{44}+(C_{11}-C_{12}-2C_{44})\cos(4\theta)(u+v')] \\ & +32h^2(C_{11}-C_{12}-2C_{44})\cos(4\theta)(v'-u'')+8a^2h^2\rho(\ddot{v}'-\ddot{u}'')+16(C_{11}-C_{12}-2C_{44})h^2\sin(4\theta)(v''-u''') \\ & +2h^2[3C_{11}+C_{12}+2C_{44}+(C_{11}-C_{12}-2C_{44})\cos(4\theta)](u''-v''')\}=0 \end{aligned} \tag{21a}$$

$$\begin{aligned} Y_2 = {} & \frac{bh}{96a^3}\{4a^2\rho[2(12a^2+h^2)\ddot{v}-2h^2\ddot{u}'] \\ & +4(C_{11}-C_{12}-2C_{44})\sin(4\theta)[24a^2u+2(12a^2+h^2)v'-2h^2u''] \\ & -[3C_{11}+C_{12}+2C_{44}+(C_{11}-C_{12}-2C_{44})\cos(4\theta)]\times[24a^2u'+2(12a^2+h^2)v''-2h^2u''']\}=0 \end{aligned} \tag{21b}$$

Obviously, Eqs. (21a) and (21b) are a set of partial differential equations with coefficients being functions of the circumferential variable θ. If the ring is made of polycrystalline silicon instead of single crystalline silicon, then the two governing equations above will become a set of partial differential equations with constant coefficients by using the condition $C_{44} = (C_{11}-C_{12})/2$.

4. The solution of equations of vibration

It is an extremely difficult task to get exact solutions of Eqs. (21) by solving them using the method of separation variables. Some authors (Eley et al., 1999; Fox et al., 1999; Hwang et al., 1999) solved their own particular problems by assuming that pairs of mode shapes of an anisotropic ring are the same as those of an isotropic ring as

$$\begin{Bmatrix} u \\ v \end{Bmatrix} \approx \begin{Bmatrix} n\sin n\theta \\ \cos n\theta \end{Bmatrix} \quad \text{and} \quad \begin{Bmatrix} u \\ v \end{Bmatrix} \approx \begin{Bmatrix} n\cos n\theta \\ -\sin n\theta \end{Bmatrix} \tag{22}$$

The mode shapes of an anisotropic ring are assumed in the form of $\sin n\theta$ and $\cos n\theta$ as those of the isotropic ring is a good approach because they guarantee not only the single-value functions at $\theta = 0$ and $\theta = 2\pi$, but also the derivatives of any order of the displacement functions with respect to θ are continuous at these two points. Another concern is that there is no proof about the issue that the proportional ratio of radial to tangential displacements of an anisotropic ring remains the same as $n/1$ shown in Eq. (22) of an isotropic ring. We will assume that the pair of mode shapes of the anisotropic ring are the same as those of the isotropic ring but with the amplitude (or proportional) ratio kept unknown. Thus the displacements of one of the pair of the nth flexural modes (which is also called the nth cosine mode) are of the form

$$\begin{Bmatrix} u(\theta,t) \\ v(\theta,t) \end{Bmatrix} = \begin{Bmatrix} X_1(t)\cos n\theta \\ X_2(t)\sin n\theta \end{Bmatrix} \tag{23}$$

Since the partial differential Eqs. (21) are linear and smooth, the solution is unique. If the solution of the equations obtained by plugging the assumed form of displacements (23) into those governing equations indeed exists, according to the unique-

ness of solution, then this solution for displacements is the only solution of what we want. (Precisely speaking, displacement functions (23) and (36) which are given later on, form a basis for the space of solution of the partial differential Eqs. (21)).

The independent variables θ and t are kept fixed when taking variation on the dependent variables (such as the generalized coordinates X_1 and X_2), thus we have

$$\begin{cases} \delta u = \cos n\theta\, \delta X_1 \\ \delta v = \sin n\theta\, \delta X_2 \end{cases} \tag{24}$$

Now substituting Eqs. (24), (21a) and (21b) into Eq. (20) and integrating θ from 0 to 2π gives

$$\int_{t_0}^{t_1} \left[\int_0^{2\pi} F_1(\theta; X_1, X_2) \mathrm{d}\theta \right] \delta X_1 \mathrm{d}t + \int_{t_0}^{t_1} \left[\int_0^{2\pi} F_2(\theta; X_1, X_2) \mathrm{d}\theta \right] \delta X_2 \mathrm{d}t = 0. \tag{25}$$

Since these two variations, δX_1 and δX_2, of generalized coordinates are arbitrary, their coefficients $\int_0^{2\pi} F_1(\theta; X_1, X_2)\mathrm{d}\theta$ and $\int_0^{2\pi} F_2(\theta; X_1, X_2)\mathrm{d}\theta$ must be zero. After integration with respect to θ, we obtain the governing equations of generalized coordinates $X_1(t)$ and $X_2(t)$ as

$$\begin{aligned} &\frac{bh\sin(4n\pi)}{48a^3 n(n^2-4)}\{-[C_{12}+2C_{44}-(n^2-3)C_{11}][(12a^2+n^4h^2)X_1+n(12a^2+n^2h^2)X_2]\} \\ &\quad+\frac{bh}{48a^3 n}\{n\pi(3C_{11}+C_{12}+2C_{44})(12a^2+h^2n^4)X_1+n^2\pi(3C_{11}+C_{12}+2C_{44})(12a^2+h^2n^2)X_2 \\ &\quad+a^2\rho[\sin(4n\pi)+4n\pi][(12a^2+h^2n^2)\ddot{X}_1+nh^2\ddot{X}_2]\}=0 \end{aligned} \tag{26a}$$

$$\begin{aligned} &\frac{bh\sin(4n\pi)}{48a^3 n(n^2-4)}\{n[C_{12}+2C_{44}+(n^2-5)C_{11}][(12a^2+h^2n^2)X_1+n(12a^2+h^2)X_2]\} \\ &\quad+\frac{bh}{48a^3 n}\{-n^2\pi(3C_{11}+C_{12}+2C_{44})(12a^2+h^2n^2)X_1-n^3\pi(3C_{11}+C_{12}+2C_{44})(12a^2+h^2)X_2 \\ &\quad+a^2\rho[\sin(4n\pi)-4n\pi][nh^2\ddot{X}_1+(12a^2+h^2)\ddot{X}_2]\}=0 \end{aligned} \tag{26b}$$

Therefore, the original set of partial differential equations, Eqs. (21), with variable coefficients are converted to the set of ordinary differential equations, Eqs. (26), with constant coefficients.

There is a factor, $\sin 4n\pi/(n^2-4)$, appearing in the first term of the LHS of Eqs. (26a) and (26b). It comes from one of the several alike integrations contained in $\int_0^{2\pi} F_i(\theta; X_1, X_2)\mathrm{d}\theta, i = 1, 2$, such as

$$\int_0^{2\pi} A(X_1, X_2) \times \cos n\theta \times \cos n\theta \times \cos 4\theta\, \mathrm{d}\theta = \frac{nA}{4}\frac{\sin 4n\pi}{(n^2-4)}. \tag{27a}$$

The value of this integration is zero when $n \neq 2$. However, it is finite when $n = 2$ and can be obtained by using L'Hospital's rule as

$$\lim_{n\to 2}[\sin 4n\pi/(n^2-4)] = \pi \tag{27b}$$

The solution of Eq. (26) is of the form

$$X_1(t) = A\mathrm{e}^{i\omega_{nc}t} \quad \text{and} \quad X_2(t) = B\mathrm{e}^{i\omega_{nc}t} \tag{28}$$

where ω_{nc} is the natural frequency of the nth cosine mode of the ring. Substituting this into Eqs. (26a) and (26b) results in a set of algebraic amplitude equations

$$\begin{bmatrix} M_{11} & M_{12} \\ M_{21} & M_{22} \end{bmatrix} \begin{bmatrix} A \\ B \end{bmatrix} = \begin{bmatrix} 0 \\ 0 \end{bmatrix} \tag{29}$$

where the matrix elements M_{ij} are functions of natural frequencies ω_{nc}, elastic moduli C_{jk}, and geometric parameters. The non-trivial solutions of Eq. (29) require that

$$\det \begin{bmatrix} M_{11} & M_{12} \\ M_{21} & M_{22} \end{bmatrix} = 0 \tag{30}$$

Expanding Eq. (30) gives the algebraic equation

$$H_1 + \left[H_2 + H_3 \times \left(\frac{\sin(4n\pi)}{(n^2-4)} \right) \right] \times \frac{\sin(4n\pi)}{(n^2-4)} = 0 \tag{31}$$

where H_i, $i = 1,2,3$ are functions of natural frequencies ω_{nc} and are list in Appendix D. If $n = 2$, then by using L'Hospital's rule Eq. (31) becomes

$$H_1(\omega_{nc}) + [H_2(\omega_{nc}) + H_3(\omega_{nc}) \times \pi] \times \pi = 0 \tag{32}$$

Solving Eq. (32) gives the natural frequencies of the second cosine mode in the explicit form as

$$\omega_{nc1(n=2)},\omega_{nc2(n=2)}=\frac{1}{4}\sqrt{\frac{(7C_{11}+C_{12}+2C_{44})}{a^2(12a^2+5h^2)\rho}}\left[(60a^2+29h^2)\mp\sqrt{(12a^2+h^2)(300a^2+121h^2)}\right] \tag{33}$$

where the "−" sign in the square root corresponds to $\omega_{nc1(n=2)}$ and the "+" sign is associated with $\omega_{nc2(n=2)}$. If $n\neq 2$, equation. (32) reduces to

$$H_1(\omega_{nc})=0 \tag{34}$$

Solving Eq. (34) gives the natural frequencies as

$$\omega_{nc1(n\neq 2)},\omega_{nc2(n\neq 2)}=\frac{1}{2\sqrt{2}}\left\{\sqrt{\frac{(3C_{11}+C_{12}+2C_{44})}{a^2\rho[12a^2+h^2(1+n^2)]}}\times\sqrt{\{[12a^2(n^2+1)+h^2(2n^4-n^2+1)]\mp\Gamma_n\}}\right. \tag{35a, b}$$

where

$$\Gamma_n=\sqrt{(12a^2+h^2)[h^2(1-3n^2)^2+12a^2(1+n^2)^2]} \tag{35c}$$

Similarly, the "−" sign is associated with the frequency $\omega_{nc1(n\neq 2)}$ and the "+" sign associated with $\omega_{nc2(n\neq 2)}$. ω_{nc1} and ω_{nc2} in Eq. (35) are the natural frequencies of the nth cosine mode. Although they correspond to the same mode shape, they have different physical meanings: ω_{nc1} is the frequency of the mode with the central line of the ring being inextensible, while ω_{nc2} is the frequency of the mode with the central line extensible. It is obvious from Eq. (35) that ω_{nc1} is smaller than ω_{nc2}. Usually we excite the ring into vibration in frequency ω_{nc1} rather than ω_{nc2}, because the smaller the frequency is, the larger the vibration amplitude is, and the more tractable the vibration detection is.

The natural frequency of the second one of the pair of the nth flexural modes (which is also called the nth sine mode) can also be calculated in a similar way. For the nth sine mode, the radial and tangent displacements are assumed to be of the form

$$\left\{\begin{array}{l}u(\theta,t)\\ v(\theta,t)\end{array}\right\}=\left\{\begin{array}{l}X_3(t)\sin n\theta\\ X_4(t)\cos n\theta\end{array}\right\} \tag{36}$$

The natural frequency associated with this sine mode for the ring made of isotropic materials is equal to that of the cosine mode given by Eq. (23). But the same frequency of these two modes will split when the ring is made of anisotropic materials. We want to evaluate the difference in frequencies between these two modes. Substituting the variation of displacements, $\delta u=\sin n\theta\delta X_3$ and $\delta v=\cos n\theta\delta X_4$, into Eq. (20) results in a set of governing equations of the generalized coordinates $X_3(t)$ and $X_4(t)$. The solutions of the generalized coordinates are of the form

$$X_3(t)=Ce^{i\omega_{ns}t},\quad \text{and}\quad X_4(t)=De^{i\omega_{ns}t} \tag{37}$$

where ω_{ns} is the natural frequency of the nth sine mode of the ring. Substituting Eq. (37) into the governing equations of $X_3(t)$ and $X_4(t)$ gives the algebraic equation of frequency ω_{ns}

$$K_1+\left[K_2+K_3\times\left(\frac{\sin(4n\pi)}{(n^2-4)}\right)\right]\times\frac{\sin(4n\pi)}{(n^2-4)}=0 \tag{38}$$

Through symbolic calculation it is found that

$$K_1(\omega)=H_1(\omega),\quad K_2(\omega)=-H_2(\omega),\quad K_3(\omega)=H_3(\omega) \tag{39}$$

For the case where $n=2$, Eq. (38) becomes

$$K_1+(K_2+K_3\times\pi)\times\pi=0 \tag{40}$$

The explicit form expressions of natural frequencies of the second sine mode can be obtained from solving Eq. (40)

$$\omega_{ns1(n=2)},\omega_{ns2(n=2)}=\frac{1}{4}\sqrt{\frac{(5C_{11}+3C_{12}+6C_{44})}{a^2(12a^2+5h^2)\rho}}\times\sqrt{\left[(60a^2+29h^2)\mp\sqrt{(12a^2+h^2)(300a^2+121h^2)}\right]} \tag{41a, b}$$

By comparing Eq. (41) with Eq. (33), we find that, for $n=2$, the natural frequencies of the sine mode described by Eq. (36) are different to those of the cosine mode defined by Eq. (23). This is mainly due to the fact that $K_2\neq H_2$ as can be seen from Eq. (39).

Now for the case where $n\neq 2$, Eq. (38) reduces to $K_1(\omega_{ns})=0$. Solving this equation gives

$$\omega_{ns1(n\neq 2)}=\omega_{nc1(n\neq 2)}\quad\text{and}\quad\omega_{ns2(n\neq 2)}=\omega_{nc2(n\neq 2)} \tag{42}$$

This means that the natural frequencies of the sine mode are equal to those of the cosine mode for any value of n except when $n=2$, because $K_1(\omega)=H_1(\omega)$.

Since for the ring made of isotropic material the cosine and sine modes have the same natural frequency and these two modes are called a pair of degenerated modes, now we want to check whether ω_{ns} equates ω_{nc} when the ring made of single

silicon crystal is replaced by the one made of polycrystalline silicon. Using $C_{44} = (C_{11} - C_{12})/2$, the factor $(7C_{11} + C_{12} + 2C_{44})$ in Eq. (33) becomes $8C_{11}$ and the factor $(5C_{11} + 3C_{12} + 6C_{44})$ in Eq. (41) also becomes $8C_{11}$. Thus the splitting frequencies ω_{ns} and ω_{nc} are reconciled. For the ring made of polycrystalline silicon, combining the expressions for natural frequencies of the ring with the central line being inextensible for $n = 2$ and all other $n \neq 2$ cases yields

$$\omega_{nc1} = \omega_{ns1} = \left\{ \sqrt{\frac{C_{11}}{2a^2\rho[12a^2 + h^2(1+n^2)]}} \times \sqrt{\{[12a^2(n^2+1) + h^2(2n^4 - n^2 + 1)] - \Gamma_n\}} \right. \tag{43}$$

Similarly, the natural frequencies of flexural vibration of the Si(1 1 1) ring can also be obtained in the explicit form as

$$\omega_{nc1}(=\omega_{ns1}), \omega_{nc2}(=\omega_{ns2}) = \sqrt{\frac{\overline{C}_{11}}{2a^2\rho[12a^2 + h^2(1+n^2)]}} \times \sqrt{\{[12a^2(n^2+1) + h^2(2n^4 - n^2 + 1)] \mp \Gamma_n\}} \tag{44a, b}$$

where the value of $\overline{C}_{11}$ is given in Appendix C.

The difference between Eqs. (44) and (43) is that the elastic constant C_{11} in Eq. (43) is replaced by $\overline{C}_{11}$ in Eq. (44). The reason is that polycrystalline silicon is fully isotropic, but Si(1 1 1) is not three-dimensionally isotropic but only in-plane (two-dimensional) isotropic. Both polycrystalline silicon ring and Si(1 1 1) ring do not exhibit frequency splitting phenomena.

To find the ratio of tangential to radial displacements, we substitute Eq. (33) or (35) into Eq. (29) to obtain the amplitude ratio of the nth cosine mode

$$\frac{B}{A} = -\frac{2n[12a^2 + (2n^2 - 1)h^2]}{(12a^2 + h^2)(n^2 - 1) + \Gamma_n} \tag{45a}$$

Similarly, the amplitude ratio of the nth sine mode can be obtained as

$$\frac{D}{C} = -\frac{B}{A} \tag{45b}$$

Eqs. (45a) and (45b) reveal that the ratio of tangential to radial displacements of an anisotropic ring depends on the ring size and on the number n of the nth flexural mode. It should be noted that the ratio is the same regardless of the elastic moduli. If the ring is of high aspect-ratio (i.e. $a \gg h$ and $a \gg b$), the ratios of tangential to radial displacements of the nth cosine and sine flexural modes of the anisotropic ring can be approximated as

$$\frac{B}{A} \approx -\frac{1}{n} \quad \text{and} \quad \frac{D}{C} \approx \frac{1}{n} \tag{46}$$

which are the same as those of the isotropic ring (Love, 1944).

Natural frequencies of pairs of similar modes of the ring made of single-crystal silicon wafers that are cut parallel to the (1 0 0) and (1 1 1) planes, and made of polycrystalline silicon wafer are calculated by using the explicit equations obtained here. The dimensions of the ring are given in Table 1. The elastic constants of Si(1 0 0), Si(1 1 1), and polycrystalline silicon, are given in Table 2, where $\overline{C}'_{11}$, $\overline{C}'_{12}$, and $\overline{C}'_{66}$ are the elements of the stiffness matrix $\mathbf{C}_{(1\,1\,1,\theta)}$ and their values are given in Appendix C. Substituting these elastic constants into Eqs. (34), (35), (41), (43) and (44) gives the values of natural frequencies of the ring as shown in Table 3.

Now we make an attempt to give the physical explanation of why the natural frequencies, ω_{nc} and ω_{ns}, of pairs of similar modes are different for the $n = 2$ flexural mode but the same for all other pairs. In Fig. 7, the mode shapes and the Young's

Table 1
The dimensions of the ring

Parameter	Value
Ring density	$\rho = 2330$ kg/m^3
Ring radius	$a = 5000$ μm
Ring thickness	$h = 50$ μm
Ring height	$b = 150$ μm

Table 2
Material parameters of silicon wafer

Single-crystal (Si(1 0 0))		Ploy-crystal (silicon)		Single-crystal (Si(1 1 1))		Unit
Parameters	Value	Parameters	Value	Parameters	Value	
C_{11}	165.7	C_{11}	165.7	$\overline{C}'_{11}$	194.4	GPa
C_{12}	63.9	C_{12}	63.9	$\overline{C}'_{12}$	54.333	GPa
C_{44}	79.6	C_{44}	50.9	$\overline{C}'_{66}$	70.0333	GPa

Table 3
The natural frequencies of a silicon ring

n	Single-crystal (Si(100) ring)		Ploy-crystal (Si(100) ring)		Single-crystal (Si(111) ring)		Unit
	ω_{nc}	ω_{ns}	ω_{nc}	ω_{ns}	ω_{nc}	ω_{ns}	
2	13,344	13,887	13,064	13,064	14,150	14,150	rad/s
3	38,517	38,517	36,950	36,950	40,022	40,022	rad/s
4	73,851	73,851	70,846	70,846	76,737	76,737	rad/s
5	119,428	119,428	114,570	114,570	124,096	124,096	rad/s
6	175,190	175,190	168,064	168,064	182,038	182,038	rad/s

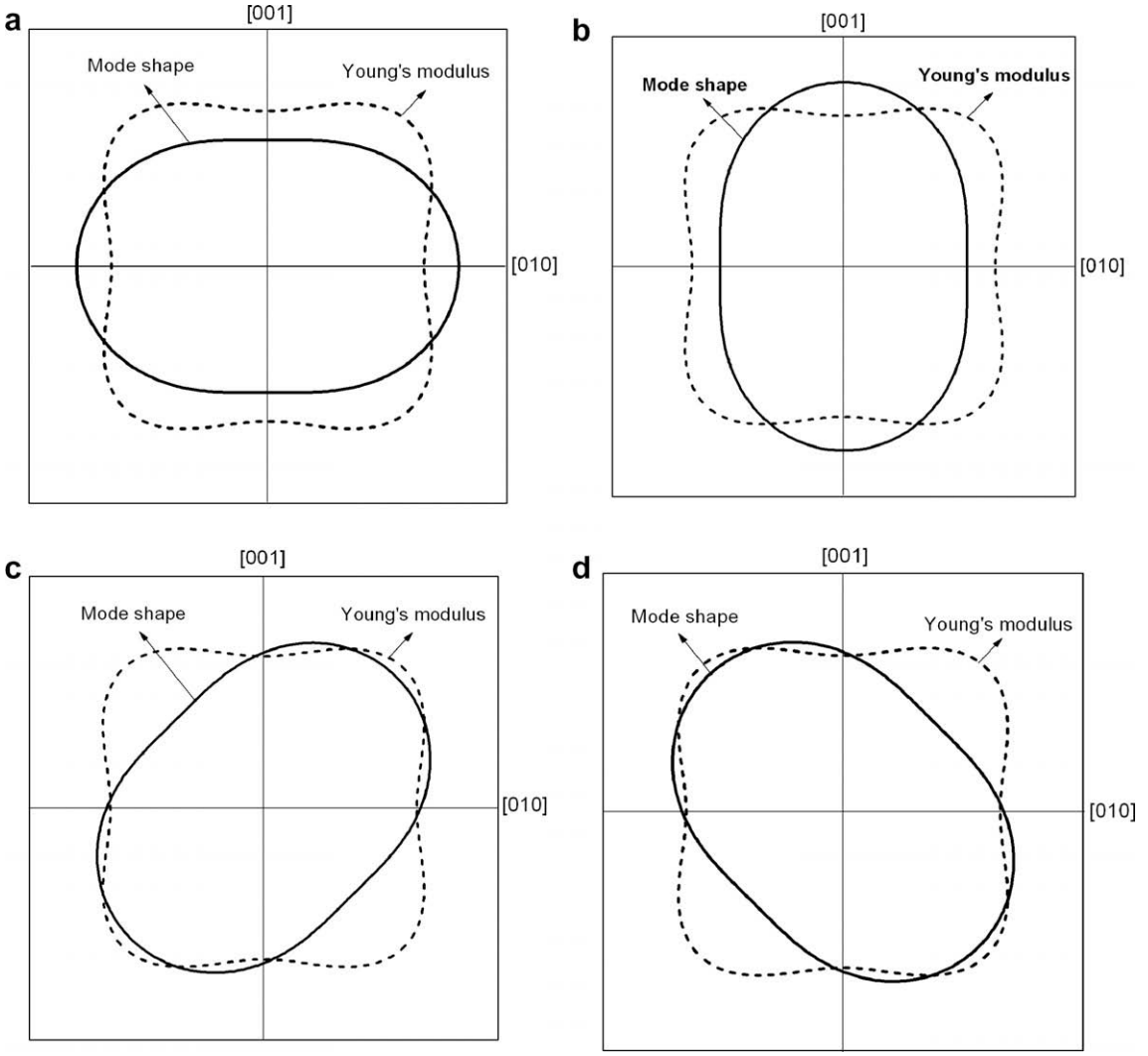

Fig. 7. (a) The ring of cos 2θ mode stretches in the vertical direction. (b) The ring shown in (a) rebounds to stretch in the horizontal direction. (c) The ring of sin 2θ mode stretches toward the ring's points of most strong stiffness. (d) The rebound of the ring shown in (c).

modulus of the Si(100) ring for the $n = 2$ case, which both are functions of θ, are plotted on the same chart. It is clear that for the cos 2θ mode the maximum stretch and rebound of the ring is in the direction along the points of the ring with least stiffness; while for the sin 2θ mode the ring stretches and rebounds to its maximum extent in the direction along the points with most stiffness. With recourse to the simple concept that, for a spring-mass-dashpot system of mass m and stiffness k, the natural frequency is proportional to the square root of k such that $\omega = \sqrt{k/m}$. Therefore, the natural frequency of the cos 2θ mode must be less than that of the sin 2θ mode; this is truly reflected in Table 3:ω_{nc} (=13,344 rad/s for $n = 2$) is less than ω_{ns}(=13,887 rad/s for $n = 2$).

Now we turn to Fig. 8. The stretch and rebound of the ring for the cos 3θ mode is shown on the left-hand side of Fig. 8 and those for the sin 3θ mode on the right-hand side. It should be noted that, if we rotate the mode shapes of the cos 3θ mode clockwise by an angle of 90°, the orientations of the mode shapes relative to the Young's modulus curve are found to be exactly the same as those for the sin 3θ mode. This is the reason why the natural frequencies of these two modes are equal. But, how does this 90° rotation symmetry come? Since single-crystal silicon is a face-centered diamond structure (Kittel, 2005), according to the classification of point symmetry group, it belongs to the class of $m3m$. A symmetry operation will take the crystal structure into itself, that is, the original pattern of atomic arrangement is indistinguishable from that of the final pattern after symmetry operation. The symmetry elements of point group $m3m$ contains six diad axes, three tetrad axes, a centre and four triads axes. All of these can be produced by putting mirrors parallel to both {1 1 0} and {1 0 0} coupled with the four triad axes (McKie and McKie, 1986; Kelly et al., 2000). One of these three tetrad axes is the [0 0 1] axis. Thus the initial state of a silicon crystal is identical to its final state after a rotation about the [0 0 1] axis (or the z-axis of Fig. 5) by an angle of 90°. This is also the reason why the Young's modulus has a 90° rotation symmetry. Hence, if one rotates the ring together with the cos 3θ mode shape clockwise by an 90° angle about the z-axis, he will find the rotated mode shape is exactly the same the sin 3θ mode shape. Therefore, the frequency of cos 3θ mode must be equal to that of sin 3θ modes, because they have the same atomic arrangement. This 90° rotation symmetry also happens to the fifth ($n = 5$) flexural mode. If the mode shapes in Fig. 9(a) and (b) denote the stretch and rebound of cos 5θ mode, and those in Fig. 9(c) and (d) represent the stretch and rebound of sin 5θ mode, it is clear that after a 90° rotation about the z-axis, the orientation of the cos 5θ mode shape (Fig. 9(a)) relative to the Young's modulus become that of the sin 5θ mode shape (Fig. 9(c)) relative to the Young's modulus. This phenomenon of a 90° rotation symmetry also happens to the mode shapes shown in Fig. 9(b) and (d). Thus we conclude that both frequencies of cos 5θ and sin 5θ modes are equal.

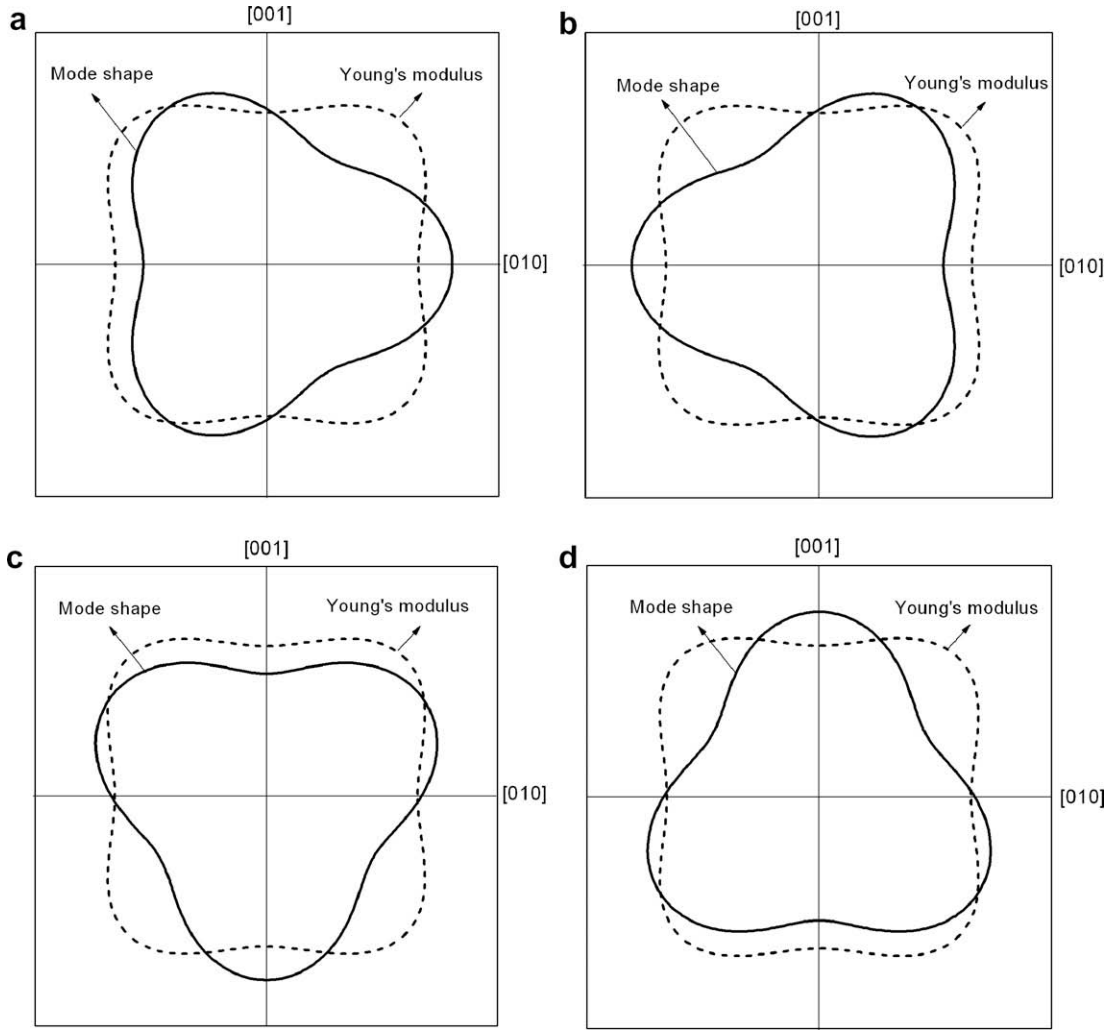

Fig. 8. (a) and (b) show the stretch and rebound of the cos 3θ mode. (c) and (d) show the stretch and rebound of the sin 3θ mode.

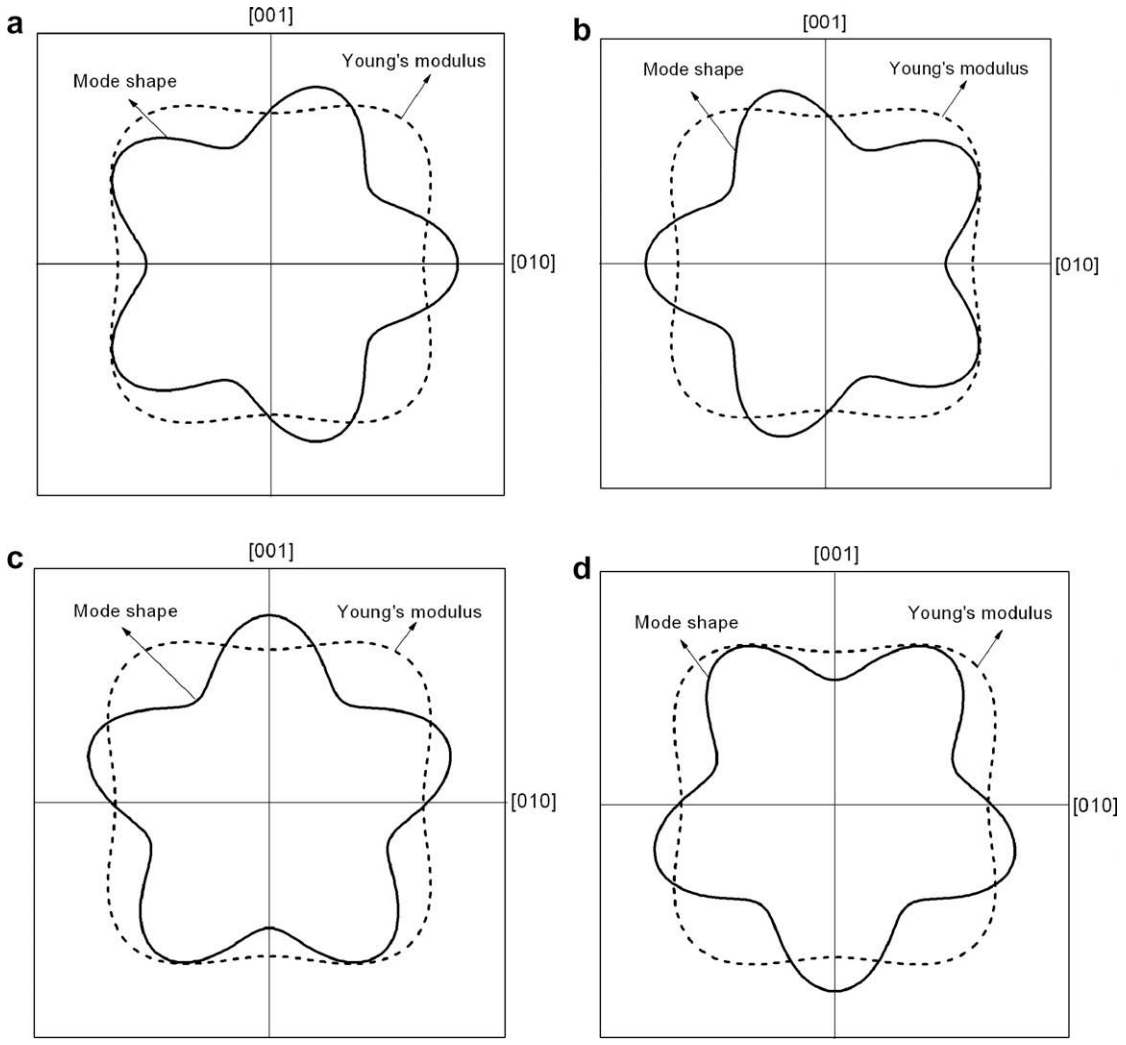

Fig. 9. (a) and (b) show the stretch and rebound of cos 5θ mode. (c) and (d) show the stretch and rebound of the sin 5θ mode.

The orientations of the mode shapes of cos 4θ and sin 4θ modes with respect to the Young's modulus are shown in Fig. 10. The in-plane crystallographic 90° rotation symmetry can not be applied to explain the equality of natural frequencies for these two modes. Unlike the cos 2θ mode where the maximum stretch of the ring always occurs at the zone which is the least stiff as can be seen in Fig. 7(a) and (b), the maximum stretch in the first half period of oscillation occurs at the zone which is the least stiff (Fig. 10(a)). However, in the other half period, the maximum stretch occurs in the place which is the most stiff (Fig. 10(b)); therefore, in the average sense over a period the strain energy of the cos 4θ may be equal to that of the sin 4θ mode where both the maximum stretch (Fig. 10(c)) and maximum rebound (Fig. 10(d)) occur at the region of moderate stiffness. Similarly, the equality in frequency for other pairs of similar modes is due to the reason that *they have the same averaged strain energy over one period*. This can be proved rigorously in the following.

Let $E_c(\omega_{nc})$ denote the total energy of the ring which is in free vibration in cos $n\theta$ mode with natural frequency ω_{nc}, and then we have $E_{nc}(\omega_{nc}) = K_{nc} + V_{nc}$, where K_{nc} is the kinetic energy and V_{nc} the strain energy. Now if the ring is set into free vibration in the other mode instead, says, the sin $n\theta$ mode with frequency ω_{ns} but with the same total energy as that of the cos $n\theta$ mode. We want to prove that $\omega_{ns} = \omega_{nc}$ for all the modes except for the $n = 2$ one.

We assume that the amplitudes of these two modes described by Eqs. (28) and (37) are the same because their assumed total energies are the same, that is, $A = C$ and $B = D$. Let the notation "$\langle\rangle$" denote the operator averaging over one period. Then

$$\langle E_{nc}(\omega_{nc})\rangle = \langle K_{nc}\rangle + \langle V_{nc}\rangle \tag{47}$$

where

$$\langle K_{nc}\rangle = \frac{1}{T_{nc}}\int_0^{T_{nc}}\left[\int_0^{2\pi}\int_{-b/2}^{b/2}\int_{-h/2}^{h/2}\frac{\rho}{2}a(\vec{v}_p\cdot\vec{v}_p)d\bar{r}\mathrm{d}z\mathrm{d}\theta\right]\mathrm{d}t, \tag{48a}$$

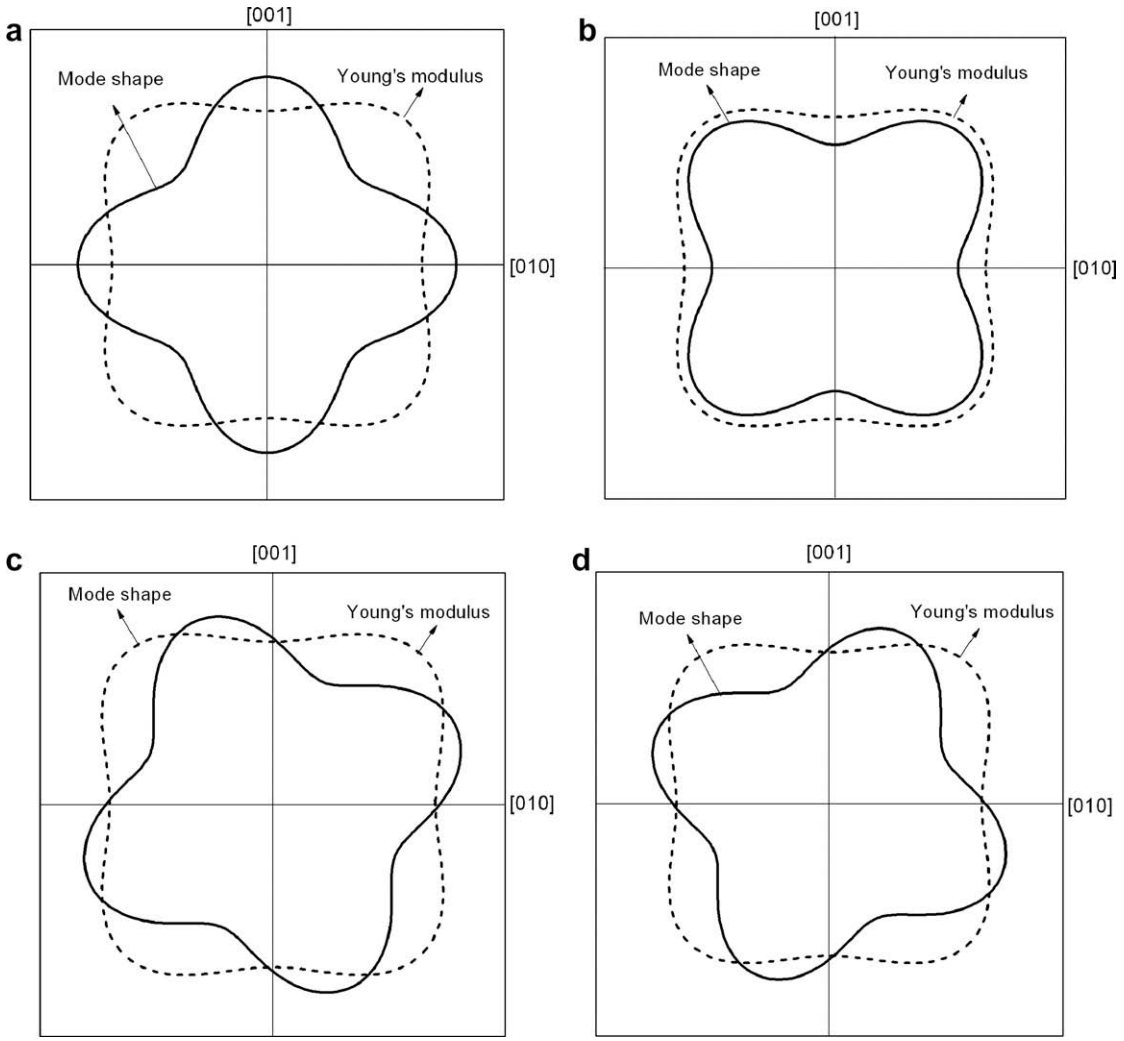

Fig. 10. (a) and (b) show the stretch and rebound of the cos 4θ mode and (c) and (d) show the stretch and rebound of the sin 4θ mode.

and $T_{nc} = 2\pi/\omega_{nc}$. Similarly

$$\langle V_{nc}\rangle = \frac{1}{T_{nc}}\int_0^{T_{nc}}\left[\int_0^{2\pi}\int_{-b/2}^{b/2}\int_{-h/2}^{h/2}\frac{a}{2}(\boldsymbol{\varepsilon}^{\mathbf{T}}\mathbf{C}\boldsymbol{\varepsilon})d\bar{r}\mathrm{d}z\mathrm{d}\theta\right]\mathrm{d}t \tag{48b}$$

Through calculating Eqs. (15) and (18) and using Eq. (45), the averaged kinetic and strain energy of the cos $n\theta$ and sin $n\theta$ modes for the nth in-plane flexural modes with $n \neq 2$ are obtained as

$$\langle K_{nc}(\omega_{nc})\rangle_{n\neq 2} = \frac{A^2 bh\pi\rho\omega_{nc}^2}{96an^2}\Delta_{n1} \tag{49a}$$

$$\langle V_{nc}\rangle_{n\neq 2} = -\frac{A^2 bh\pi(3C_{11}+C_{12}+2C_{44})}{384a^3(12a^2+h^2)}\Delta_{n2} \tag{49b}$$

$$\langle K_{ns}(\omega_{ns})\rangle_{n\neq 2} = \frac{C^2 bh\pi\rho\omega_{ns}^2}{96an^2}\Delta_{n1} \tag{49c}$$

$$\langle V_{ns}\rangle_{n\neq 2} = -\frac{C^2 bh\pi(3C_{11}+C_{12}+2C_{44})}{384a^3(12a^2+h^2)}\Delta_{n2} \tag{49d}$$

where

$$\Delta_{n1} = 12a^2(1+n^2)^2 - \frac{h^2(3n^2-1)}{12a^2+h^2}\times(h^2-3n^2h^2+\Gamma_n) + 12a^2[h^2(1-3n^2)^2-(n^2-1)\times\Gamma_n]$$

$$\Delta_{n2} = -144a^4(n^2+a)^2 + h^2(3n^2-1)\times(h^2-3n^2h^2+\Gamma_n) + 12a^2[-2h^2(1-2n^2+5n^4)+(1+n^2)\times\Gamma_n]$$

and Γ_n is defined by Eq. (35c).

By observing Eqs. (49b) and (49d) we know that, if the two different free vibrations, one is in cos $n\theta$ mode and the other in sin $n\theta$ mode, have the same total mechanical energy, that is, $A = C$, the averaged strain energy over their own period of these two modes is the same for all the ($n \neq 2$) cases and is independent of the frequency. Then from $\langle E_{nc}(\omega_{nc})\rangle = \langle E_{ns}(\omega_{ns})\rangle$, we have $\langle K_{nc}(\omega_{nc})\rangle_{n\neq 2} = \langle K_{ns}(\omega_{ns})\rangle_{n\neq 2}$. Also from Eqs. (49a) and (49c) we know $\omega_{nc} = \omega_{ns}$ for all the n except $n = 2$.

Now we consider the $n = 2$ case, the averaged kinetic and strain energy can be obtained in the similar way

$$\langle K_{nc}(\omega_{nc})\rangle_{n=2} = \frac{A^2 bh\rho\pi\omega_c^2}{384a(12a^2+h^2)} \times \Delta_{n3} \tag{50a}$$

$$\langle V_{nc}\rangle_{n=2} = 9A^2 bh^3\pi(7C_{11}+C_{12}+2C_{44}) \times \Delta_{n4} \tag{50b}$$

$$\langle K_{ns}(\omega_{ns})\rangle_{n=2} = \frac{A^2 bh\rho\pi\omega_s^2}{384a(12a^2+h^2)} \times \Delta_{n3} \tag{50c}$$

$$\langle V_{ns}\rangle_{n=2} = 9C^2 bh^3\pi(5C_{11}+3C_{12}+6C_{44}) \times \Delta_{n4} \tag{50d}$$

where

$$\Delta_{n3} = 3600a^4 + a^2(1752h^2 - 36\Lambda) + 11h^2(11h^2 - \Lambda)$$

$$\Delta_{n4} = \frac{(300a^2+121h^2)}{16a[3600a^4 + 11h^2(11h^2+\Delta) + 12a^2(146h^2+5\Delta)]}$$

and $\Lambda = \sqrt{(12a^2+h^2)(300a^2+121h^2)}$.

It is clear that, although the amplitudes of vibration of the pair of second flexural modes are equal, their strain energies are not equal due to the anisotropic effect. Based on the assumed equal mechanical energy, we have that $\langle K_{nc}(\omega_{nc})\rangle_{n=2} \neq \langle K_{ns}(\omega_{ns})\rangle_{n=2}$. This leads to the result that $\omega_{nc} \neq \omega_{ns}$ for the $n = 2$ case and therefore, the phenomenon of frequency splitting only happens to the second flexural mode.

5. Conclusions

This work presents the analysis of in-plane free vibration of rings made of single-crystal silicon wafers cut parallel to the (100) and (111) planes. It is the anisotropic elastic constants appearing in the strain energy that causes the equations of motion of the vibrating ring, derived using Hamilton's principle, into a set of partial differential equations with coefficients being periodic in polar variable. These partial differential equations with varying coefficients are then converted into a set of ordinary differential equations by assuming that the mode shapes are the same as those of the isotropic ring but with non-predetermined amplitude. The natural frequencies and amplitude of mode shapes are solved exactly in the explicit form. If the ring is made of a Si(100) wafer, the elastic constants are fully anisotropic; any pair of similar modes remain degenerate, which means that the two natural frequencies of that pair are equal, except for the second ($n = 2$) flexural mode. The phenomena of frequency splitting and degeneration of pairs of similar modes are explained based on the crystallographic symmetry elements of single-crystal silicon and the conservation of the averaged total energy. If the ring is made of a Si(111) wafer, the elastic constants are in-plane isotropic but out-of-plane anisotropic. It is found that the mode shapes depend only on the size and modal number of the ring, and they are all the same no matter what the ring is made of, Si(100), or Si(111), or poly-crystalline silicon. Finally, when the ring is of high aspect ratio, i.e. the radius is much larger than the height and width, the ratio of radial to tangential displacements equals to $1/n$ for the cos $n\theta$ flexural mode and $-1/n$ for the sin $n\theta$ flexural mode.

Acknowledgement

The research work was sponsored by National Science Council of Republic of China under the Contract number NSC95-2221-E-002-040-MY2 and is acknowledged gratefully.

Appendix A. Stiffness and Compliance matrix elements of Si(100)

The rotation matrix **A** which rotates the rectangular coordinate system X, Y, Z about the Z axis by an angle θ into the cylindrical coordinate system r, θ, z is

$$\mathbf{A} = [a_{ij}] = \begin{bmatrix} \cos\theta & \sin\theta & 0 \\ -\sin\theta & \cos\theta & 0 \\ 0 & 0 & 1 \end{bmatrix}$$

The stiffness matrix with respect to this cylindrical coordinates can be obtained by using the tensor transformation Eq. (3). For example, the matrix coefficient C'_{11} is given by

$$\begin{aligned} C'_{11} &= C'_{1111} = a_{1m}a_{1n}a_{1o}a_{1p}C_{mnop} \\ &= a_{11}a_{11}a_{11}a_{11}C_{1111} + a_{11}a_{11}a_{12}a_{12}C_{1122} + a_{12}a_{12}a_{11}a_{11}C_{2211} + a_{11}a_{12}a_{11}a_{12}C_{1212} + a_{12}a_{12}a_{12}a_{12}C_{2222} \end{aligned}$$

Using Eq. (1) for subscript conversion, the symmetric property $C_{ijkl} = C_{klij}$, and the equality $C_{22} = C_{11}$ and $C_{66} = C_{44}$ for Si(1 0 0), the above equation becomes

$$\begin{aligned} C'_{11} &= \cos^4\theta\, C_{11} + 2\cos^2\theta \sin^2\theta C_{12} + \sin^4\theta C_{11} + \sin^2\theta\cos^2\theta C_{44} \\ &= \frac{1}{4}[3C_{11} + C_{12} + 2C_{44} + (C_{11} - C_{12} - 2C_{44})\cos 4\theta]. \end{aligned} \tag{A1}$$

The other coefficients of the stiffness matrix $\mathbf{C}'_{(1\,0\,0,\theta)}$ are

$$\begin{aligned} C'_{12} &= \frac{1}{4}[C_{11} + 3C_{12} - 2C_{44} - (C_{11} - C_{12} - 2C_{44})\cos 4\theta] \\ C'_{13} &= C_{12} \\ C'_{16} &= -\frac{1}{4}(C_{11} - C_{12} - 2C_{44})sin4\theta \\ C'_{26} &= \frac{1}{4}(C_{11} - C_{12} - 2C_{44})\sin 4\theta \\ C'_{33} &= C_{11} \\ C'_{44} &= C_{44} \\ C'_{66} &= \frac{1}{4}[C_{11} - C_{12} + 2C_{44} - (C_{11} - C_{12} - 2C_{44})\cos 4\theta] \end{aligned} \tag{A2}$$

The relationship between stiffness matrix and compliance matrix elements for cubic system is

$$S_{11} = \frac{C_{11} + C_{12}}{(C_{11} - C_{12})(C_{11} + 2C_{12})}, \quad S_{12} = \frac{-C_{12}}{(C_{11} - C_{12})(C_{11} + 2C_{12})} \quad S_{44} = 1/C_{44}. \tag{A3}$$

Then the compliance matrix element of $S'_{(1\,0\,0,\theta)}$ in term of S_{ij} are

$$\begin{aligned} S'_{11} &= \frac{1}{8}[6S_{11} + 2S_{12} + S_{44} + (2S_{11} - 2S_{12} - S_{44})\cos 4\theta] \\ S'_{12} &= \frac{1}{8}[2S_{11} + 6S_{12} - S_{44} - (2S_{11} - 2S_{12} - S_{44})\cos 4\theta] \\ S'_{13} &= S_{12} \\ S'_{16} &= -\frac{1}{4}(2S_{11} - 2S_{12} - S_{44})\sin 4\theta \\ S'_{26} &= \frac{1}{4}(2S_{11} - 2S_{12} - S_{44})\sin 4\theta \\ S'_{33} &= S_{11} \\ S'_{44} &= S_{44} \\ S'_{66} &= \frac{1}{2}[2S_{11} - 2S_{12} + S_{44} - (2S_{11} - 2S_{12} - S_{44})\cos 4\theta] \end{aligned} \tag{A4}$$

Appendix B. The elastic and shear moduli of Si(1 0 0)

Here we rederive the Young's and shear moduli from the compliance coefficients given by Wortman and Evans (1965) in order to verify Eqs. (5a) and (5c). When we rotate the rectangular coordinate system XYZ about an arbitrary direction with the origin fixed into the coordinate system $\bar{X}\bar{Y}\bar{Z}$, the components in coordinates $\bar{X}\bar{Y}\bar{Z}$ are related to those in coordinates XYZ by

$$\begin{Bmatrix} \bar{X} \\ \bar{Y} \\ \bar{Z} \end{Bmatrix} = \begin{bmatrix} l_1 & m_1 & n_1 \\ l_2 & m_2 & n_2 \\ l_3 & m_3 & n_3 \end{bmatrix} \begin{Bmatrix} X \\ Y \\ Z \end{Bmatrix} \tag{B1}$$

where l_i, m_i, and n_i are the direction cosines of the transformation. Wortman and Evans (1965) derived the compliance and stiffness coefficients for cubic system as functions of direction cosines as follows:

$$
\begin{aligned}
S'_{11} &= S_{11} + \left(S_{11} - S_{12} - \frac{1}{2}S_{44}\right)(l_2^4 + m_2^4 + n_2^4 - 1)\\
S'_{33} &= S_{11} + \left(S_{11} - S_{12} - \frac{1}{2}S_{44}\right)(l_3^4 + m_3^4 + n_3^4 - 1)\\
S'_{44} &= S_{44} + 4\left(S_{11} - S_{12} - \frac{1}{2}S_{44}\right)(l_2^2 l_3^2 + m_2^2 m_3^2 + n_2^2 n_3^2)\\
S'_{66} &= S_{44} + 4\left(S_{11} - S_{12} - \frac{1}{2}S_{44}\right)(l_2^2 l_1^2 + m_2^2 m_1^2 + n_2^2 n_1^2)
\end{aligned}
\tag{B2}
$$

If the coordinate system is rotated about the Z axis, then we have

$$
\begin{bmatrix} \cos & \sin\theta & 0 \\ -\sin\theta & \cos\theta & 0 \\ 0 & 0 & 0 \end{bmatrix} = \begin{bmatrix} l_1 & m_1 & n_1 \\ l_2 & m_2 & n_2 \\ l_3 & m_3 & n_3 \end{bmatrix}, \tag{B3}
$$

Substituting Eq. (B3) into Eq. (B2) gives the elements of compliance matrix for Si(1 0 0) as

$$
\begin{aligned}
S'_{11} &= S_{11} - \frac{1}{4}\left(S_{11} - S_{12} - \frac{1}{2}S_{44}\right)(1 - \cos 4\theta)\\
S'_{33} &= S_{11} - \left(S_{11} - S_{12} - \frac{1}{2}S_{44}\right)\\
S'_{44} &= S_{44}\\
S'_{66} &= S_{44} + \left(S_{11} - S_{12} - \frac{1}{2}S_{44}\right)(1 - \cos 4\theta)
\end{aligned}
\tag{B4}
$$

These results are equal to those in Eqs. (5a) and (5c).

Appendix C. Elements of stiffness and compliance matrices of Si(1 1 1)

The non-zero entries of stiffness matrix $\mathbf{C}'_{(1\,1\,1)}$ are

$$
\begin{aligned}
\overline{C}_{11} &= \frac{(C_{11} + C_{12} + 2C_{44})}{2}, \quad \overline{C}_{12} = \frac{(C_{11} + 5C_{12} - 2C_{44})}{6},\\
\overline{C}_{13} &= \frac{(C_{11} + 2C_{12} - 2C_{44})}{3}, \quad \overline{C}_{15} = \frac{(C_{11} - C_{12} - 2C_{44})}{3\sqrt{2}},\\
\overline{C}_{33} &= \frac{(C_{11} + 2C_{12} + 4C_{44})}{3}, \quad \overline{C}_{44} = \frac{(C_{11} - C_{12} + C_{44})}{3},\\
\overline{C}_{66} &= \frac{(C_{11} - C_{12} + 4C_{44})}{6}
\end{aligned}
\tag{C1}
$$

The elements of the stiffness matrix $\mathbf{C}_{(1\,1\,1,\theta)}$ are

$$
\begin{aligned}
&\overline{C}'_{11} = \overline{C}_{11}, \quad \overline{C}'_{12} = \overline{C}_{12},\\
&\overline{C}'_{13} = \overline{C}_{13}, \quad \overline{C}'_{15} = \overline{C}_{15}\cos\theta[2\cos 2\theta - 1],\\
&\overline{C}'_{24} = \overline{C}_{15}\sin\theta[2\cos 2\theta + 1], \quad \overline{C}'_{33} = \overline{C}_{33},\\
&\overline{C}'_{44} = \overline{C}_{44}, \quad \overline{C}'_{66} = \overline{C}_{66}
\end{aligned}
\tag{C2}
$$

The elements of compliance matrix $S_{(1\,1\,1,\theta)}$ are

$$
\begin{aligned}
\overline{S}'_{11} &= \frac{\overline{C}_{15}^2\overline{C}_{33} + \overline{C}_{44}(\overline{C}_{13}^2 - \overline{C}_{11}\overline{C}_{33})}{[2\overline{C}_{13}^2 - \overline{C}_{33}(\overline{C}_{11} + \overline{C}_{12})][\overline{C}_{44}(\overline{C}_{11} - \overline{C}_{12}) - 2\overline{C}_{15}^2]}\\
\overline{S}'_{12} &= \frac{\overline{C}_{13}^2\overline{C}_{44} - \overline{C}_{33}(\overline{C}_{15}^2 + \overline{C}_{12}\overline{C}_{44})}{[2\overline{C}_{13}^2 - \overline{C}_{33}(\overline{C}_{11} + \overline{C}_{12})][\overline{C}_{44}(\overline{C}_{11} - \overline{C}_{12}) - 2\overline{C}_{15}^2]}\\
\overline{S}'_{13} &= \frac{\overline{C}_{13}}{2\overline{C}_{13}^2 - \overline{C}_{33}(\overline{C}_{11} + \overline{C}_{12})}, \quad \overline{S}'_{15} = \frac{\overline{C}_{15}\cos 3\theta}{2\overline{C}_{15}^2 - \overline{C}_{44}(\overline{C}_{11} - \overline{C}_{12})},\\
\overline{S}'_{24} &= \frac{\overline{C}_{15}\sin 3\theta}{2\overline{C}_{15}^2 - \overline{C}_{44}(\overline{C}_{11} - \overline{C}_{12})}, \quad \overline{S}'_{33} = \frac{\overline{C}_{11} + \overline{C}_{12}}{\overline{C}_{33}(\overline{C}_{11} + \overline{C}_{12}) - 2\overline{C}_{13}^2},\\
\overline{S}'_{44} &= \frac{\overline{C}_{11} - \overline{C}_{12}}{\overline{C}_{44}(\overline{C}_{11} - \overline{C}_{12}) - 2\overline{C}_{15}^2}, \quad \overline{S}'_{66} = \frac{\overline{C}_{44}}{\overline{C}_{44}\overline{C}_{66} - \overline{C}_{15}^2}.
\end{aligned}
\tag{C3}
$$

Appendix D. The coefficients $H_i(\omega_{nc})$ in Eq. (31)

The coefficients $H_i(\omega_{nc})$ given in Eq. (31) are

$$H_1(\omega_{nc}) = \frac{\pi^2 b^2 h^2 e^{2i\omega_{nc}t}}{192a^4}\{(3C_{11}+C_{12}+2C_{44})^2 h^2 (n-n^3)^2 - 4a^2(3C_{11}+C_{12}+2C_{44})[12a^2(1+n^2)+h^2(1-n^2+2n^4)]\rho\omega_{nc}^2 + 16a^4[12a^2+h^2(1+n^2)]\rho^2\omega_{nc}^4\} \tag{D1}$$

$$H_2(\omega_{nc}) = \frac{n\pi b^2 h^2 e^{2i\omega_{nc}t}}{192a^4}\{(C_{11}-C_{12}-2C_{44})\times[2(3C_{11}+C_{12}+2C_{44})h^2(-1+n^2)^2 - a^2(-12a^2(-9+n^2)+h^2(1+7n^2))\rho\omega_{nc}^2]\} \tag{D2}$$

$$H_3(\omega_{nc}) = \frac{b^2 h^2 e^{2i\omega_{nc}t}}{192a^4}\{-h^2(-1+n^2)^2[C_{11}(-5+n^2)+C_{12}+2C_{44}][C_{11}(-3+n^2)-C_{12}-2C_{44}] + \frac{1}{n^2}\langle a^2h^2(-4+n^2)\rho\omega_{nc}^2[(C_{12}+2C_{44})(-1+n)(1+n)+C_{11}(-3+4n^2-9n^4+2n^6)]\rangle - \frac{12a^6(-4+n^2)^2\rho^2\omega_{nc}^4}{n^2} + \frac{1}{n^2}\langle a^4(-4+n^2)\rho\omega_{nc}^2\times[12(C_{12}+2C_{44})(-1+n^2) + 12C_{11}(-3+4n^2+n^4)-h^2(-4-3n^2+n^4)\rho\omega_{nc}^2]\rangle\} \tag{D3}$$

References

Ashcroft, N.W., Mermin, N.D., 1975. Solid State Physics. Saunders College Publishing.

Ayazi, F., Najafi, K., 2001. A HARPASS polysilicon vibrating ring gyroscope. Journal of Microelectromechanical Systems 10 (1), 169–179.

Bickford, W.B., Reddy, E.S., 1985. On the in-plane vibration of rotating rings. Journal of Sound and Vibration 101 (1), 13–22.

Brantley, W.A., 1973. Calculated elastic constants for stress problems associated with semiconductor devices. Journal of Applied Physics 44 (1), 534–536.

Carrier, G.F., 1945. On the vibrations of a rotating ring. Quarterly Applied Mathematics 3, 235–245.

Eley, R., Fox, C.H.J., McWilliam, S., 1999. Anisotropy effects on the vibration of circular rings made from crystalline silicon. Journal of Sound and Vibration 228 (1), 11–35.

Elwenspoek, M., Jansen, H.V., 1998. Silicon Micromachining. Cambridge University Press.

Fox, C.H.J., Hwang, R.S., McWilliam, S., 1999. The in-plane vibration of thin rings with in-plane profile variations. Part II. Application to nominally circular rings. Journal of Sound and Vibration 220 (3), 517–539.

He, G., Najafi, K., 2002. A single-crystal silicon vibrating ring gyroscope. In: Proceedings of the International Conference on Micro Electro Mechanical Systems (MEMS 2002), pp. 718–721.

Hopkins, I.D., 1997. Performance and design of a silicon micro-machined gyro. In: Proceedings of the DGON Symposium on Gyro Technology, Stuttgart.

Hwang, R.S., Fox, C.H.J., McWilliam, S., 1999. The in-plane vibration of thin rings with in-plane profile variations. Part I. General background and theoretical formulation. Journal of Sound and Vibration 220 (3), 497–516.

Kelly, A., Groves, G.W., Kidd, P., 2000. Crystallography and Crystal defects. Wiley.

Kim, W., Chung, J., 2002. Free non-linear vibration of a rotating thin ring with the in-plane and out-of-plane motions. Journal of Sound and Vibration 258 (1), 167–178.

Kirkhope, J., 1976. Simple frequency expression for the in-plane vibration of thick circular rings. Journal of the Acoustial Society of America 59, 86–89.

Kirkhope, J., 1977. In-plane vibrations of thick circular rings. Journal of Sound and Vibration 50, 219–227.

Kittel, C., 2005. Introduction to Solid State Physics, Eighth ed. Wiley.

Lee, S.Y., Chao, J.C., 2000. Out-of-plane vibrations of curved non-uniform beams of constant radius. Journal of Sound and Vibration 238 (3), 443–458.

Love, A.E.H., 1944. A Treatise on the Mathematical Theory of Elasticity, Fourth ed. Dover, New York.

Mal, A.K., Singh, S.J., 1991. Deformation of elastic solids. Prentice-Hall, New Jersey.

McKie, D., McKie, C., 1986. Essentials of Crystallography. Blackwell Scientific Publications.

Nye, J.F., 1957. Physical Properties of Crystals, their Representation by Tensors and Matrices. Oxford Science Publications.

Putty, M.W., Najafi, K., 1994. A Micromachined Ring Gyroscope. In: Proceedings of the Solid State Sensor and Actuator Workshop, pp. 213–220.

Reismann, H., Pawlik, P.S., 1980. Elasticity, Theory and Applications. Wiley, New York.

Royer, D., Dieulesaint, E., 2000. Elastic Waves in Solids I. Springer.

Shuvalov, L.A., 1981. Modern Crystallography. IV. Physical Properties of Crystals. Springer, New York.

Tang, C.S., Bert, C.W., 1987. Out-of-plane vibrations of thick rings. International Journal of Solids and Structures 23 (1), 175–185.

Wortman, J.J., Evans, R.A., 1965. Young's modulus, shear modulus, and Poisson's ratio in silicon and germanium. Journal of Applied Physics 36 (1), 153–156.